JOURNAL OF MATERIALS SCIENCE 14 (1979) 966–974

Mechanical properties and surface defects of boron fibres prepared in a closed CVD system

JAN-OTTO CARLSSON, TORSTEN LUNDSTRÖM
Institute of Chemistry, University of Uppsala, Box 531, S-751 21 Uppsala, Sweden

The tensile strength of boron fibres, prepared on a tungsten wire substrate suspended in a closed CVD system, has been investigated. The influence of strain-rate, gauge length, and fibre diameter on the tensile fracture stress of the fibres has been evaluated and compared to fracture stress data of fibres produced in continuous CVD processes. Moreover, the *E*-modulus of the prepared fibres has been measured. Finally the surface defects of the fibres have been examined and classified into fracture stress depressive surface defects and non-fracture stress depressive surface defects.

1. Introduction

The excellent mechanical properties and the low density of boron fibres make them an attractive alternative in fibre-strengthened materials, particularly in light-weight constructions. Boron fibres are utilized, for instance, in commercial aircraft and sports equipment. Normally the boron fibre consists of a tungsten boride core surrounded by a boron mantle. The various techniques of boron fibre preparation as well as methods of increasing the fracture stress of boron fibres after production have recently been reviewed [1].

The continuous production of boron fibres is usually performed in open CVD reactors, with the substrate tungsten wire entering and leaving through mercury seals at each end. The seals also serve as electrical contacts. The seals have the disadvantage of contaminating the fibre and causing hot spots to develop on the fibre. Moreover, when the fibre is drawn through the seals, it is quenched rapidly, introducing thermal stresses into the fibre. All these effects weaken the fibre. In the present investigation the mechanical properties of boron fibres produced in a closed CVD system without such seals were studied. The CVD system used allows the fibres to be prepared at different total pressures, different mechanical loads and different cooling rates after interrupting the preparation process.

2. Experimental details

2.1. Preparation of boron fibres

The closed CVD system used for the boron fibre preparation has been described in detail elsewhere [2] and only a brief description of the experimental procedure is given here. A 14 μm thick tungsten filament is suspend over two tungsten rods, which are at a distance of 16 cm apart in a horizontal deposition chamber. In order to keep the filament straight it is loaded with 0.2 g weights at each end. The filament is heated to 1280° C for 5 min in hydrogen (66.5 kPa) to reduce tungsten oxides on the filament surface and to remove surface contaminants such as graphite particles from the filament drawing process. After the hydrogen treatment, the deposition chamber is evacuated and flushed several times with hydrogen. The reaction gas mixture, containing hydrogen and boron trichloride in a predetermined molar ratio, is then introduced into the depositon chamber to a pressure of 66.5 kPa. The deposition chamber is then closed and the filament heated.

Preparation of boron fibres at constant temperature cannot be carried out in this or the continuous process. Fig. 1 shows a typical temperature/time curve, recorded during a boron fibre preparation in the present closed CVD system. The temperature decrease (T_{dec}, see Fig. 1), i.e. the difference between the maximum temperature and

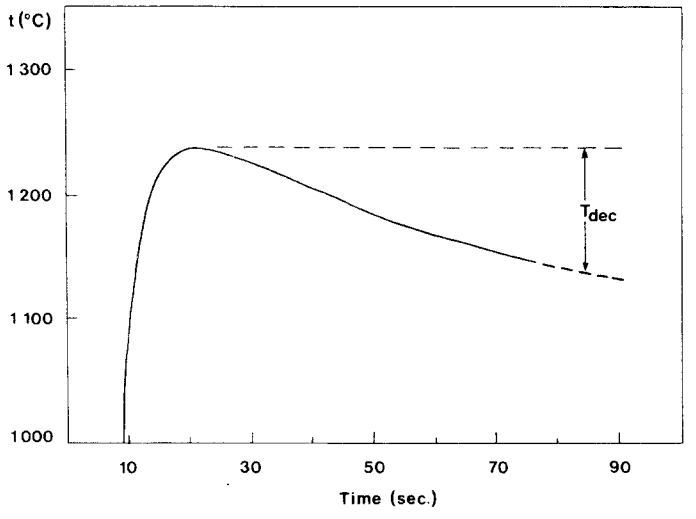

Figure 1 Recorded temperature/time curve during a boron fibre preparation in a closed CVD system.

the temperature at the end of the fibre preparation, depends among other things on the rise time of the current through the filament and the molar ratio of the reactants. The longer the rise time and the higher the boron trichloride content in the gas mixture the smaller is the temperature decrease after attainment of maximum temperature. The rise time used was equal for all reaction gas mixtures and it was chosen to give the smallest possible temperature decrease, T_{dec}. Table I shows the temperature decrease, T_{dec} for two different maximum temperatures (1230 and 1160° C) and for different molar ratios between hydrogen and boron trichloride at a total pressure of 66.5 kPa. In addition, fibre diameters as well as preparation times are given. The temperatures are corrected for absorption in glass and for the emissivity of the boron deposit [2]. It is seen from Table I, that the largest temperature decreases and the longest preparation times are obtained in gas mixtures with high hydrogen/boron trichloride molar ratios.

Inclusions and crystalline areas initiate fracture at low stresses in boron fibres. By utilizing high-purity gases in the preparation process inclusions can be eliminated while fibre crystallization can be avoided by a suitable choice of temperature and time. The boron trichloride used contained at least 99.8% boron trichloride and the claimed purity of the hydrogen used is specified in Table II. The high nitrogen content is due to the fact that the vessels used in the analytical work were flushed several times with nitrogen prior to analysis. The concentrations of other contaminants in the hydrogen are very low and are further reduced by passing the gas through a liquid nitrogen cold trap, before admission to the reaction chamber.

TABLE II Claimed purity of hydrogen used in present study

Substance	H_2O	O_2	N_2	CO	CO_2	Cl_2	C_2H_4	CH_4	H_2S
Conc. (ppm)	6	1	115	1	2	0.2	1	1	1

2.2. Tensile testing

The fibres were tested at 22° C in a micro-tensile testing machine (Alwetron TCS-100) and in an Instron testing machine. In order to reduce the slippage between the pneumatic metal grips and the fibre, emery paper and a relatively high gripping pressure (20 to 50 MN m^{-2}) were used.

In the fracture stress measurements, the gauge lengths and the strain-rates were in the ranges 10 to 120 mm and 2.78 x 10^{-3} to 11.1 x 10^{-3} sec^{-1}, respectively. The fibre diameters were measured to an accuracy of ± 0.5 μm in a metal microscope with back-lighting. A small number of the fibres employed for the fractographic investigations were mounted between a sheet of paper and adhesive

TABLE I Preparation data of boron fibres

T_{max} (° C)	Molar ratio H_2/BCl_3	T_{dec} (° C)	Time (sec)	Diameter (μm)
1230	3/2	100	60	139
1230	5/1	70	61	134
1230	10/1	135	90	105
1230	20/1	200	93	93
1160	3/2	150	120	128
1160	5/1	100	90	108
1160	10/1	170	177	93
1160	20/1	250	300	80

TABLE III Tensile fracture stress data of boron fibres

Strain-rate (10^3 sec^{-1})	Gauge length (mm)	Diameter (μm)	Number of tests	Average fracture stress (GN m^{-2})	S.D. (GN m^{-2})
2.78	30	108.0	13	3.2	0.7
4.17	30	108.0	16	3.3	0.5
5.56	30	108.0	14	3.2	0.6
8.33	30	108.0	13	3.4	0.5
11.1	30	108.0	14	3.4	0.6
2.78	30	85.2	14	3.2	0.8
2.78	30	94.9	13	3.3	0.7
2.78	30	114.4	14	3.4	0.6
2.78	30	126.7	15	3.4	0.6
8.33	10	108.0	13	3.5	0.5
2.78	60	108.0	13	2.9	0.8
2.78	120	108.0	15	2.7	0.7

tape for the tensile testing [3] to retain the pieces of the fibres obtained after failure.

Determination of the modulus of elasticity of boron fibres was performed from the stress–strain curve. The E-modulus can be obtained by plotting the E-modulus obtained at different gauge lengths versus the corresponding reciprocal gauge lengths, and extrapolating to zero. The boron fibres were tested at gauge lengths from 10 to 130 mm and at a strain-rate of 3×10^{-3} sec^{-1}.

2.3. Electron microscopy

The surface defects and the fracture surfaces of the boron fibres were examined in a scanning electron microscope (JSM-U3), operated at 15 to 25 kV. All the specimens were cleaned in alcohol in an ultrasonic cleaner for 10 min and then coated with gold.

3. Results and discussion

3.1. Mechanical properties

The influence of testing conditions and fibre diameters on the fracture stresses of boron fibres can be seen from Table III. All the fibres tested were prepared under the same experimental conditions. Fibres with different diameters were obtained by interrupting the preparation process at different stages.

3.1.1. The fracture stress dependence on strain-rate and fibre diameter

From Table III it is obvious that the fracture stress of boron fibres is independent of the strain-rates as well as the fibre diameters. There is a good agreement between the present results and those of Swansson and Hancock [4], who tested 102 and 142 μm thick boron fibres and observed no significant difference in fracture stress. On the other hand, Galasso *et al.* [5] observed an increase in fracture stress (2.62 to 3.13 GN m^{-2}) with increasing fibre diameter (51 to 127 μm). However, in the fibre diameter range 85 to 127 μm, i.e. the diameter range tested in the present investigation (see Table III), the fracture stress increase can be estimated from data given in [5] to about 0.2 GN m^{-2} (2.95 to 3.13 GN m^{-2}).

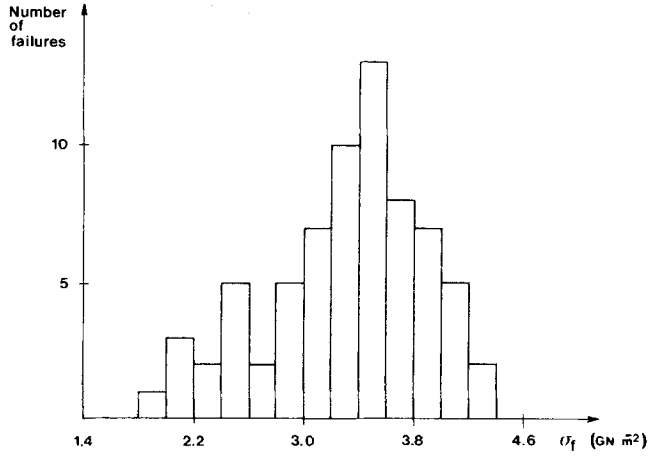

Figure 2 Histogram showing the fracture stresses of boron fibres with the same diameters tested with different strain-rates.

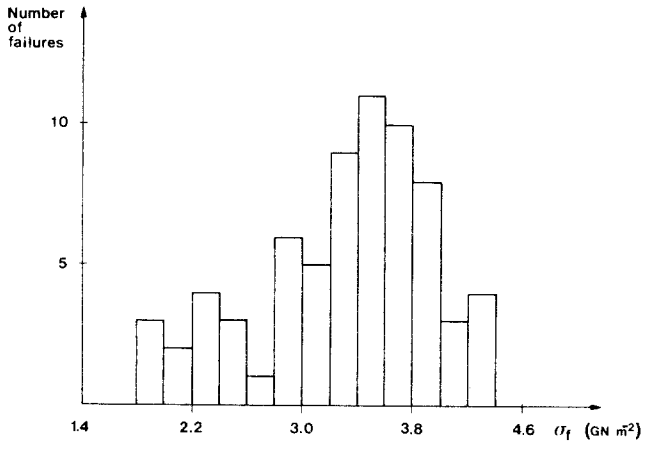

Figure 3 Histogram showing the fracture stresses of boron fibres with different diameters tested at the same strain-rate.

Since in the present investigation the fracture stresses were found to be independent of the strain-rate and fibre diameter, the strain-rate data and fibre diameter data can be summarized in the histograms shown in Figs. 2 and 3. The histograms exhibit the characteristic negatively skewed distributions obtained and discussed in [3, 4, 6, 7].

Earlier investigations [3, 6, 8, 9] have shown that the various fracture mechanisms in boron fibres can be correlated with certain fracture stress intervals. Low fracture stresses are caused by crystalline growths, radial cracks, surface flaws and inclusions, while high fracture stresses are obtained when the fractures are initiated within or very close to the tungsten boride core. Since the E-modulus of the tungsten borides in the core is higher than that of boron, considerably higher core stresses than the average fibre stresses are obtained at fracture, which is demonstrated by the calculation below.

The tungsten boride core diameter in the 108 μm thick boron fibre is 19 μm and consists of W_2B_5 and WB_4. (The boron contents of these phases are most probably lower than indicated by their ideal crystallographic formulae [10, 11]). The diameter of the W_2B_5 region is estimated to be 12 μm. DiCarlo reported to Behrendt [12], that the E-moduli of boron, WB_4 and W_2B_5 were 393, 407 and 669 GN m^{-2}, respectively. The value 669 GN m^{-2} for the E-modulus of W_2B_5 is somewhat lower than that reported by Portnoi *et al.* [13] (775 GN m^{-2}). Using the assumption of no interfacial glide between the boride core and the boron mantle, and putting the load carried by the core and mantle equal to the total load of the fibre (with $E_{WB_4} = E_B$), the following equation is obtained

$$\sigma_c = \frac{E_{W_2B_5} \cdot \sigma_f}{E_b + (E_{W_2B_5} - E_B) \cdot (D_{W_2B_5}/D_f)^2},$$

where σ_c and σ_f are the core and fibre fracture stresses, respectively, while $D_{W_2B_5}$ and D_f are the

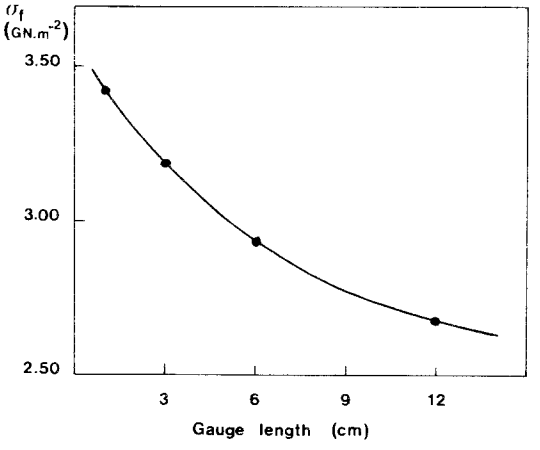

Figure 4 Average fracture stress of boron fibres as a function of gauge length.

TABLE IV The gauge length factor, σ_1/σ_{30}, at various gauge lengths obtained from different investigations

Gauge length (mm)	10	20	30	50	100
Morita *et al.* [7] σ_1/σ_{30}	1.07	1.03	1.00	0.94	0.86
Zhigach *et al.* [14]* σ_1/σ_{30}	1.10	1.03	1.00	0.93	0.85
This investigation σ_1/σ_{30}	1.07	1.03	1.00	0.97	0.91
Mean	1.08	1.03	1.00	0.95	0.87

*From the normal distribution

diameters of the W_2B_5 core and the fibre, respectively. The equation gives a core fracture stress of 6.75 GN m^{-2} for the rather high fibre fracture stress of 4.00 GN m^{-2}.

3.1.2. The fracture stress dependence on gauge length

An increased gauge length will decrease the fracture stress since the failure probability increases. This is shown in Fig. 4 and has also been observed by Morita *et al.* [7] and Zhigach *et al.* [14]. All these measurements can be compared after calculating a gauge length factor defined as the average fracture stress of the fibres at a gauge length of 1 mm (σ_1) divided by the average fracture stress of the fibres at a normalized length, in this case 30 mm (σ_{30}). The calculated gauge length factors, σ_1/σ_{30}, at various gauge lengths from the investigations mentioned above are given in Table IV. The agreement between the investigations is good, in particular at gauge lengths of 10 to 50 mm, i.e. gauge lengths normally used for mechanical testing of boron fibres. Consequently, the gauge length factor gives a reliable means of comparing fracture stress data of boron fibres measured at different gauge lengths.

3.1.3. Modulus of elasticity of boron fibres

The modulus of elasticity of the boron fibres, as determined from the stress–strain curve is 410 ± 25 GN m^{-2}. The E-moduli, determined from various gauge lengths, did not vary significantly, indicating no slippage in the grips. The anelastic strain component can be neglected under the testing conditions used [15] (room temperature, low stresses and short testing times). However, if there was any contribution to the strain from slippage in grips and anelastic deformation, too small values for the E-moduli would be obtained.

TABLE V E-moduli of boron fibres measured by different techniques

E-modulus (GN m^{-2})	Technique	Reference
442	Bend test	[16]
427	Modified bend test	[17]
389	Statical elongation test	[7]
393	Flexural internal friction	[15]
393–420*	Stress/strain curve	[5]
435	Stress/strain curve	[18]
410	Stress/strain curve	This work

*Various diameters.

The E-modulus determined is in good agreement with reported E-moduli (see Table V).

The E-modulus of the boron fibres is the average of that of the composite boron fibre, containing various tungsten borides in the core and boron in the mantle. Assuming that the fibre core only consists of W_2B_5 and WB_4 the E-modulus of the fibre, E_f, can be calculated from the equation

$$E_f = (E_{W_2B_5} - E_{WB_4})(D_{W_2B_5}/D_f)^2 + (E_{WB_4} - E_B)(D_c/D_f)^2 + E_B$$

where $E_{W_2B_5}$ E_{WB_4} and E_B are the E-moduli of W_2B_5, WB_4 and boron, respectively, and $D_{W_2B_5}$, D_c and D_f are diameters of the W_2B_5 cylinder in the core, the entire core and the whole fibre, respectively. Using DiCarlo's value of the E-moduli of W_2B_5 (669 GN m^{-2}), WB_4 (407 GN m^{-2}) and boron (393 GN m^{-2}) [12] the E-modulus of the fibres tested in this investigation (fibre diameter 108 μm and core diameter 19 μm) have been calculated for two different diameters of the W_2B_5 cyclinder in the core, namely 17 and 2 μm. The calculated E-moduli of the fibre were 399.9 and 393.5 GN m^{-2}, respectively, while the E-modulus of the boron used in this calculation was 393 GN m^{-2}. Thus the E-modulus of boron fibres is only slightly influenced by contributions from the tungsten boride core. The calculated E-values are in good agreement with the E-value measured experimentally in this investigation.

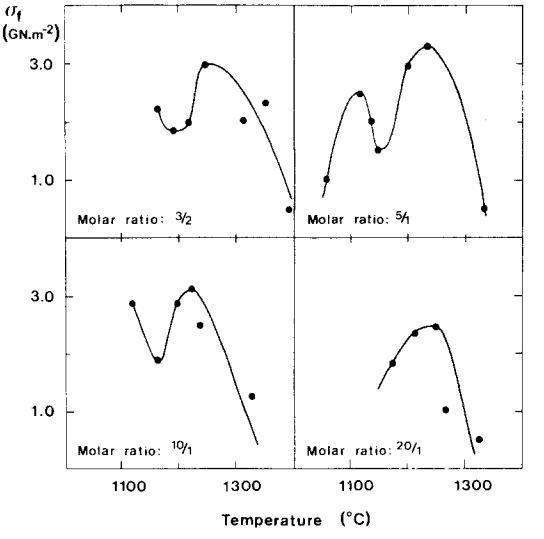

Figure 5 The tensile fracture stress as a function of the maximum deposition temperature for various molar ratios hydrogen/boron trichloride at a total pressure of 66.5 kPa.

TABLE VI Maximum average tensile fracture stresses of as-produced boron fibres from open CVD systems [4–6, 18, 19, 21] and the present closed CVD system

Average fracture stress ($GN m^{-2}$)	3.7	3.1	3.1	3.3	2.8	3.6	3.3
Reference	[4]	[5]	[6]	[18]	[19]	[21]	This work

3.1.4. Influence of deposition temperature and reaction gas composition on tensile fracture stress

The tensile fracture stress is shown as a function of the maximum deposition temperature in Fig. 5 for the molar ratios 20/1, 10/1, 5/1 and 3/2 between hydrogen and boron trichloride. The initial total pressure of the reaction gas mixture was 66.5 kPa in all cases. The standard deviations of fracture stress lie in the range 0.5 to 0.7 $GN m^{-2}$. Each fracture stress value in Fig. 5 is based on twelve to fifteen tests except those for the high temperatures (1300 to 1400° C), which are based on five to ten tests. Since the accuracy of the temperature measurements is estimated to ± 15° C [2] the temperature differences between the maxima of the curves are not significant.

Maxima in fracture stress are obtained at 1230 and 1120° C respectively, with a high-strength value of 3.3 $GN m^{-2}$ at 1230° C. At deposition temperatures above 1300 and below 1100° C, low fracture stress fibres are produced. At 1300° C the fibres display areas of crystalline boron (see Section 3.2), which weaken them considerably. At temperatures below 1100° C the preparation time is rather long, which increases the crystallinity of the fibre as well as the diameter of the tungsten boride core. Both effects reduce the fracture stress. The minima of the curves at about 1150° C are probably due to secondary nucleation of boron, reducing the fracture stress by a notch effect.

In the molar ratio range 3/2 to 10/1 approximately the same fracture stresses were observed. A molar ratio of 20/1, however, produces lower fracture stresses probably caused by the longer deposition time.

Cueilleron and Roux [19, 20] investigated the influence of deposition parameters (temperature, gas composition, etc.) on the fracture stress of boron fibres continuously produced in an open multi-stage CVD system. The largest tensile fracture stress was achieved when using one reactor only. Fibres produced, using the molar ratio range 1/1 to 10/1, displayed the same strength, which is in agreement with the present investigation. The largest fracture stress was obtained at 1030° C, which is about 200° C and 90° C, respectively, below the maxima in this investigation. However, Cueilleron and Roux measured the temperature with an optical pyrometer without applying a correction for emissivity and absorption [20]. The application of such a correction would raise the maximum temperature from 1030° C to approximately 1100° C, i.e. just near the temperature of the first maximum (1120° C) in the present investigation. A maximum corresponding to that at 1230° C was not observed by Cueilleron and Roux [19].

3.1.5. Fracture stresses of boron fibres produced in open and closed CVD systems

Published fracture stress data of boron fibres produced in open conventional CVD systems with mercury seals are shown in Table VI together with data from the present investigation. Since the gauge lengths used are normally 10 to 50 mm, correction of fracture stresses to a gauge length of, for instance, 30 mm will change the fracture stress values by less than 10% (see Section 3.1.2), which can be neglected in a rough comparison. It is evident from Table VI that the fracture stresses of boron fibres produced in open and closed CVD systems do not deviate very much from each other.

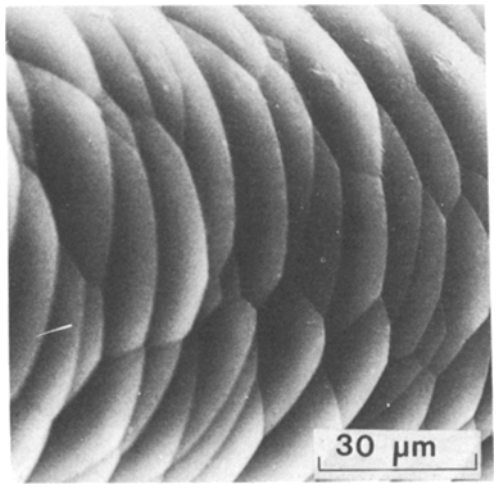

Figure 6 Characteristic morphology of a boron fibre.

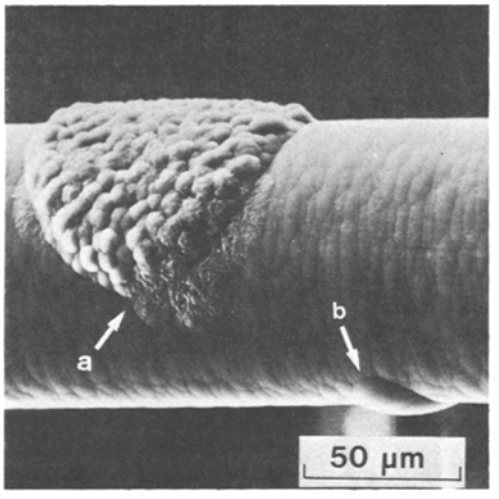

Figure 7 Crystalline boron in the boundary between two nodule morphologies (a) and an abnormal nodule (b).

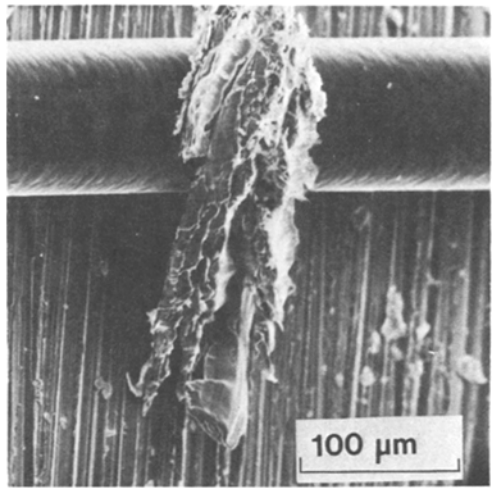

Figure 9 Photograph showing a whisker-like outgrowth.

3.2. Surface defects of boron fibres

Fig. 6 reveals the characteristic morphology of a boron fibre. Depending on the deposition conditions and the properties of the tungsten substrate various surface defects can be formed on the fibre. After tensile testing and fractographic examination of fracture surfaces, two groups of defects could be distinguished, namely fracture stress depressive surface defects (FSDS defects) and non-fracture stress depressive surface defects (NFSDS defects). Fibres with FSDS defects fracture at low stresses (0.5 to 2.5 GN m^{-2}) while fibres with NFSDS defects fracture at higher stresses (2.5 to 4.4 GN m^{-2}). In fibres with NFSDS defects fractures are usually initiated in the tungsten boride core or at the interface between the core and the boron mantle.

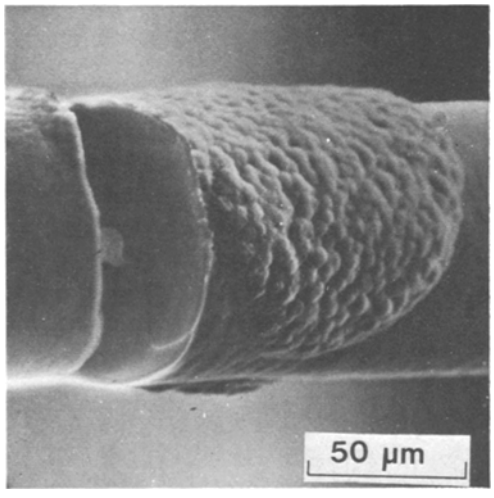

Figure 8 Fracture initiated in the crystalline boron area.

3.2.1. Fracture stress depressive surface defects

FSDS defects are shown in Figs. 7 to 9. In Fig. 7, two nodule morphologies are shown with crystalline boron in the morphology boundary. Fracture initiates in the morphology boundary (Fig. 8, fracture caused by accident in the microscope). This type of defect was obtained at higher deposition temperatures (about 1300° C) and was frequently formed on substrates with pronounced variations of diameter.

Fig. 7 also shows an abnormal nodule, probably grown around some inclusion. The abnormal nodule weakened the fibre by a notch effect to a fracture stress of about 2.4 GN m^{-2}. Fig. 9 exhibits a whisker-like outgrowth. This outgrowth (maximum ~ 1 mm) can be both an FSDS defect and an NFSDS defect. The FSDS defect was formed during the whole deposition process at areas of elevated temperatures, while the NFSDS defect was formed at the end of the process at areas of approximately the same temperature as the whole fibre.

3.2.2. Non-fracture stress depressive surface defects

Axially oriented secondary nuclei (Fig. 10) were frequently observed on fibres prepared in the closed CVD system. Nodule boundaries can form an axially oriented straight line (Fig. 11). This

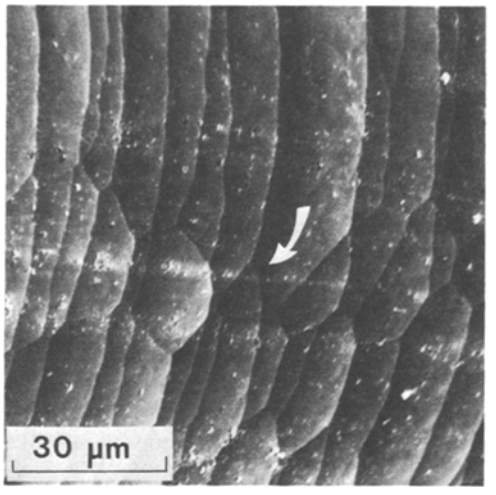

Figure 10 Axially oriented secondary nuclei.

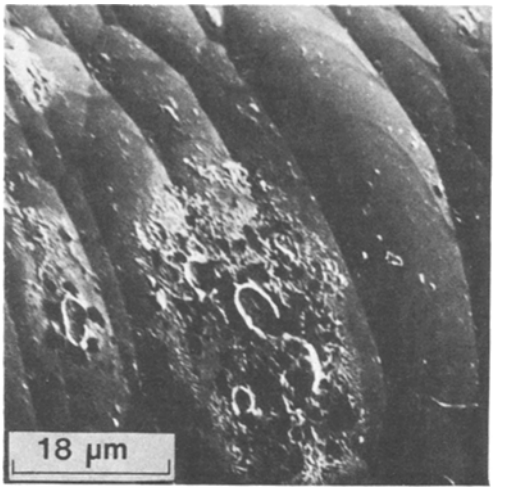

Figure 12 Crystalline areas located on the surface of the nodules.

type of defect was observed less frequently. A possible explanation for its occurrence is a simultaneous boron nucleation on neighbouring die-mark ridges on the tungsten substrate.

Small areas of crystalline boron on the fibre surface were frequently found to form on fibres prepared with long deposition times and at relatively low deposition temperatures. The crystalline areas can be located on one or on two nodules (Fig. 12) or be oriented axially (Fig. 13).

4. Conclusions

The tensile fracture stresses of boron fibres have been measured for various tensile testing conditions, deposition conditions and fibre diameters. At constant gauge length, no significant variation of fracture stress was observed in the fibre diameter range 85 to 127 μm and the strain-rate range 2.78 to 11.1×10^{-3} sec^{-1}. An increase of the gauge length causes an increased failure probability and, consequently, lower fracture stress values were obtained. The modulus of elasticity of the boron fibres investigated lies in the range previously reported in the literature (390 to 440 GN m^{-2}).

It is concluded from this investigation that fibres prepared in a closed, static CVD system have mechanical properties very similar to fibres produced continuously in an open CVD system. However, the influence of the deposition conditions on the tensile fracture stress is different for the two methods of preparation. Fibres of maximum tensile strength are produced at considerably

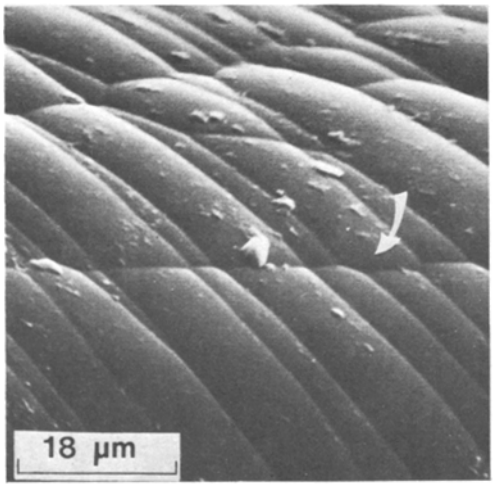

Figure 11 Nodule boundaries forming an axially oriented straight line.

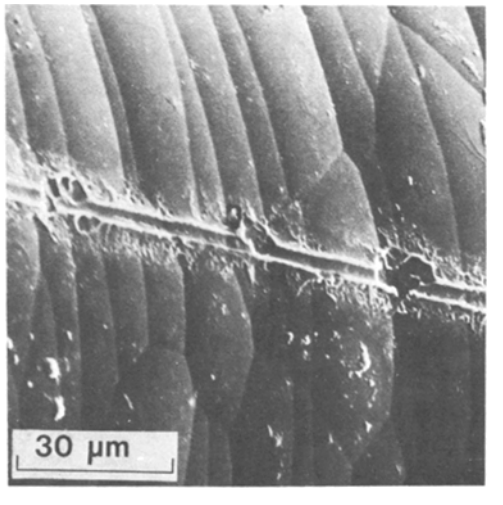

Figure 13 Axially oriented crystalline areas.

higher temperatures in a closed CVD system than in an open CVD system. Moreover, two maxima are obtained in a fracture stress/temperature curve for fibres prepared in a closed CVD system. At intermediate compositions (molar ratio H_2/BCl_3 3/2 to 10/1) no significant differences in fracture stresses of the boron fibres have been observed between fibres prepared with the two methods. However, the fracture stresses seem to decrease more rapidly with temperature at high hydrogen concentrations in a closed CVD system.

Finally, surface defects of boron fibres have been classified in fracture stress depressive surface defects and non-fracture stress depressive surface defects. From this classification and a microscopic examination of the fibre surface low fracture stress boron fibres can be identified.

Acknowledgements

The authors are grateful to Professor Stig Rundqvist for his interest and criticism of the manuscript. Thanks are due to Lumalampan AB, Stockholm, for supplying the tungsten wire. We are also indebted to Lumalampan and Fagersta Bruk AB, Fagersta, for valuable help at the tensile testing. The financial support from the Swedish Board for Technical Development is gratefully acknowledged.

References

1. J. O. CARLSSON, *J. Mater. Sci.* **14** (1979) 255.
2. *Idem, Chemica Scripta* **14** (1979) 255.
3. J. VEGA-BOGGIO and O. VINGSBO, *J. Mater. Sci.* **11** (1976) 273.
4. G. D. SWANSSON and J. R. HANCOCK, Technical Report No. 5, Contract No. N00014-70-C-0212, Midwest Research Institute, Kansas City, Missouri, USA (1972).
5. F. GALASSO, M. SALKIND, D. KUEHL and V. PATARINA, *Trans. Met. Soc. AIME* **236** (1966) 1748.
6. F. E. WAWNER, in "Modern Composite Materials", edited by L. E. Broutman and R. H. Krock (Addison Wesley, Reading, Mass, 1967) p. 244.
7. M. MORITA. H. TAKEDA and I. ARIMA, *Nippon Kinzoku Gakkaishi* **36** (1972) 1213.
8. L. E. LINE and U. V. HENDERSON, in "Handbook of Fibreglass and Advanced Plastic Composites", edited by G. Lubin (Van Nostrand Reinhold, New York, 1969).
9. G. K. LAYDEN, *J. Mater. Sci.* 8 (1973) 1581.
10. T. LUNDSTRÖM, *Arkiv Kemi* **30** (1968) 115.
11. T. LUNDSTRÖM and I. ROSENBERG, *J. Solid State Chem.* **6** (1973) 299.
12. D. R. BEHRENDT, "Composite Materials: Testing and Design" (Fourth Conference), ASTM STP 617 (American Society for Testing Materials, Philadelphia, Pa, 1977) p. 215.
13. K. I. PORTNOI, A. A. MUKUSEEV, V. N. GRIBKOV, YU. V. LEVINSSKII and S. A. PROKO'EV, *Porosh. Met.* **3** (63) (1968) 32.
14. A. F. ZHIGACH, A. M. TSIRLIN, E. A. SHCHETILINA, I. L. SVETLOV, V. I. GRIGOR'EV, E. G. SHAFRANOVICH, T. I. BULYGINA and V. A. YARTSEV, *Mekh. Polim.* **4** (1973) 641.
15. J. A. DICARLO, "Composite Materials: Testing and Design" (Fourth Conference), ASTM STP 617 (American Society for Testing Materials, Philadelphia, Pa, 1977) p. 443.
16. C. P. TALLEY, *J. Appl. Phys.* **30** (1959) 1114.
17. G. VERCHERY, *Fibre Sci. Technol.* **2** (4) (1970) 283.
18. E. G. ELLISON and D. H. BOONE, *J. Less-Common Metals* **13** (1967) 103.
19. J. CUEILLERON and Y. ROUX, *Ann. Chim.* 7 (4) (1972) 235.
20. Y. ROUX, Thesis, Lyon (1970).
21. R. J. SMITH, NASA Report TN 8219, National Aeronautics and Space Administration, Cleveland, Ohio (1976).

Received 20 July and accepted 14 September 1978.